PERGAMON

International Journal of Heat and Mass Transfer 44 (2001) 3155–3168

International Journal of HEAT and MASS TRANSFER

www.elsevier.com/locate/ijhmt

Natural convection inside ventilated enclosure heated by downward-facing plate: experiments and numerical simulations

V. Dubovsky, G. Ziskind *, S. Druckman, E. Moshka, Y. Weiss, R. Letan

Department of Mechanical Engineering, Heat Transfer Laboratory, Ben-Gurion University of the Negev, P.O. Box 653, Beer-Sheva, Israel

Received 30 May 2000; received in revised form 25 September 2000

Abstract

The present paper deals with heat transfer inside a ventilated enclosure. The enclosure is heated by a horizontal downward-facing constant-temperature hot plate. In order to provide a comprehensive picture of the problem, three main approaches are used in parallel: temperature measurement, flow visualization, and numerical simulation. The measurements are done by thermocouples distributed uniformly at the vertical mid-plane of the enclosure. The visualization is performed using the smoke of incense sticks, with video recording and consequent image processing. The computer simulations of the flow and temperature fields are performed both for steady and transient ventilation and compared with the results of the measurements and visualization. Applicability to ventilation is discussed.

Keywords: Natural convection; Closed and open enclosure; Temperature distribution; Flow field

1. Introduction

The present work is a part of an extensive study being performed in our laboratory on different aspects of passive ventilation of buildings. The major objective is to find an optimal geometry of the system, especially concerning the location of the openings. The results obtained in the experimental and numerical modeling may be used in design of low-cost and effective ventilation systems.

The problem addressed in the present work is, essentially, free convection in both closed and open enclosures. Various aspects of the flow and heat transfer inside enclosures were extensively studied in the past, and a large amount of results has been reported in the literature [1–3]. In particular, the recent results concern flow of smoke and hot gases due to a building fire [4], chimney-enhanced heat transfer from free-convection heat sinks [5], and natural convection in a three-dimensional enclosure heated by a discrete heat source [6,7]. Any heating and venting configuration is specific in nature, and the results obtained for a particular problem cannot be readily extended to cover other problems. Our study is based on measurements, flow visualization [8], and numerical calculations, performed in parallel in order to cross-examine the accuracy of the experiments and the validity of the simulations.

In the following sections, the physical model is introduced and explained. The experimental set-up is described in detail. Preliminary experiments concerning the heat-transfer coefficients are reported. Then, mapping of the temperature field and smoke visualization of the flow field are presented. The results of the measurements and visualization serve to verify and validate the numerical simulations. It is shown that the agreement between the simulations and experimental results is fairly good. This fact makes it possible to extend the numerical simulations to similar geometries. Optimal configuration of the system is discussed from the point of view of its applicability to ventilation.

* Corresponding author. Tel.: +972-7-647-7089; fax: +972-7-647-2813.

E-mail address: gziskind@gumail.bgu.ac.il (G. Ziskind).

0017-9310/01/$ - see front matter
PII: S0017-9310(00)00324-0

Nomenclature

c_p	specific heat (J/kg K)
g	gravitational acceleration (m/s^2)
h	static enthalpy (J/kg)
k	thermal conductivity (W/m K)
L	characteristic length (m)
p	pressure (Pa)
p'	modified pressure (Pa)
Ra	Rayleigh number ($= g\beta[T_p - T_m]L^3/\alpha v$)
Re	Reynolds number ($= ux/v$)
t	time (s)
T	temperature (K or °C)
u	velocity (m/s)
x	distance (m)

Greek symbols

α	thermal diffusivity (m^2/s)
β	thermal expansion coefficient (K^{-1})
μ	dynamic viscosity (kg/m s)
v	kinematic viscosity (m^2/s)
ρ	density (kg/m^3)
τ	stress tensor (N/m^2)

Subscripts

c	cover
cr	critical
i, j	component
m	mean
p	plate
r	radiation
w	wall
0	reference
∞	ambient

2. Physical model

The objective of the present study is related to ventilation of buildings. For this reason, it was quite natural to choose an enclosure in the shape of a rectangular parallelepiped. For the same reason, the walls of the enclosure are made of a material with low thermal conductivity. Heat is supplied into the enclosure by means of a hot plate, which is a part of the cover. From the point of view of the heat transfer into the enclosure, heating from above is the worst case, as heat is transferred mostly by conduction. From a practical point of view, however, the case, in which the roof is the hottest among the enclosure boundaries, is quite natural. The "roof" configuration is under investigation now. The problem where the plate is a part of a flat roof is a convenient reference base both for future experimental investigations and for verification of the computer simulations.

As a result of the temperature difference between the hot plate and other walls of the enclosure, air motion is initiated inside the enclosure. In the domain that has its windows closed, a steady state is reached when the rate of heat lost through the walls equals to the rate of heat supplied by the hot plate to the enclosure. The process of ventilation is initiated by opening the entrance and exit windows. Temperature inside the enclosure gradually decreases, until a new steady state is established.

The flow through and inside the enclosure is caused by the heat input from the plate. Accordingly, we use a thermal and flow model based on natural convection inside the enclosure. This model includes the continuity, momentum and energy equations and appropriate conditions at the boundaries. These equations will be presented later in connection with the numerical calculations.

As mentioned above, heat is supplied to the enclosure from above by means of a horizontal hot plate. This configuration has been thoroughly studied in the past. An extensive discussion of the problem, including the edge effects, can be found in Kwak and Song [9], and in Goldstein and Lau [10].

The following cases are studied in the present work:

1. The steady state which is established in the box when the entrance and exit windows are closed;
2. The steady state which is established in the box when the entrance and exit windows are open. This case is investigated for three various positions of the entrance window;
3. The transient process of ventilation, which takes place between the two above defined steady states.

In cases 1 and 2, temperature measurements and numerical calculations were performed. Case 3 was studied using smoke visualization and computer simulations. The temperature measurements gave a discrete temperature distribution in the enclosure. The numerical simulations provided the temperature field and the flow field in the enclosure.

Once the temperature field is known, it is possible to calculate the heat input from the hot plate to the system, and the heat losses to the surroundings. The induced air mass flow rate through the enclosure can be obtained either by integration of the velocity distribution through the entrance cross-section area, or from the energy balance in the open enclosure.

In addition to the convective heat transfer, radiation from the plate can take place. As a result, there is an additional heat flux coming from the plate. Since air is

transparent for thermal radiation, this flux cannot affect the inside air temperature directly. Rather, it irradiates the inner surfaces of the walls. Since the thermal resistance of the walls is very large, almost all the heat coming from the hot plate by radiation is convected to the enclosed air, thus enhancing the overall heat transfer rate from the plate to the air. As a result, the local and average temperatures in the enclosure increase.

3. Experimental study

The experiments performed in the present study include preliminary measurements of heat transfer coefficients, temperature measurements in the enclosure in closed and open states, and smoke visualization in an open enclosure.

3.1. Experimental set-up

The experimental system was designed in accordance with the physical model described above. Two experimental set-ups of the same dimensions were used: an insulated enclosure and a transparent enclosure. The transparent variant was necessary for visualization, but it was not suitable for the measurements because of its glass walls. The difference in thermal properties of the two boxes is discussed later.

The insulated enclosure, shown in Fig. 1, is a box of which overall inner length, height and width are 60, 30 and 24 cm, respectively. The box is made of two layers of cardboard, with a 20 mm layer of thermal insulation between them. The box cover is made of pressed wood, because it has to be strong enough to carry a tank of boiling water.

The heating plate is mounted flush with the downward-facing surface of the cover plate of the box. The hot plate is the bottom of a tin tank in which boiling of water is achieved by immersion of two electrical heaters, each of 600 W. The walls of the boiling tank are insulated.

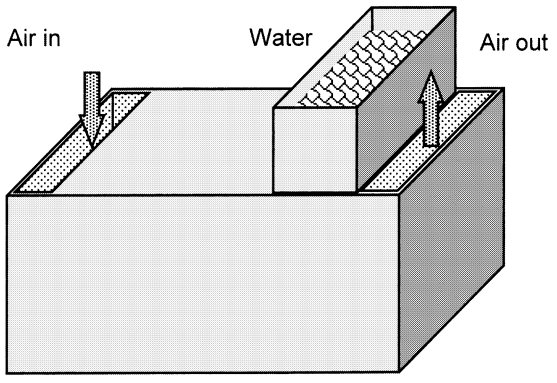

Fig. 1. General view of the experimental set-up.

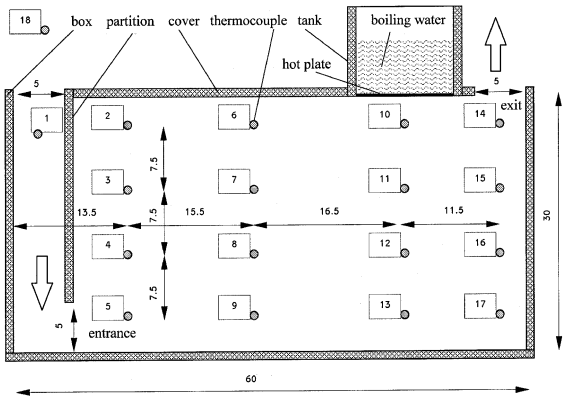

Fig. 2. Cross-section of the experimental set-up, with locations of thermocouples.

Spatial uniformity of the plate temperature was verified by a calibrated thermocouple meter. Thus, the plate temperature was constant and uniform, as expected, because the thermal resistance between the plate and the air is much larger than the resistance inside the plate and between the plate and the boiling water.

Seventeen T-type thermocouples are located as shown in Fig. 2, in the vertical mid-plane of the box. They are connected to a PC through a Fluke Hydra data acquisition unit. An additional thermocouple is used to measure the temperature of the surroundings. One can see from the figure that the row of thermocouples second from the right is placed exactly under the centerline of the hot plate. The other thermocouples are distributed uniformly in the vertical mid-plane of the box.

The cardboard box and the glass box have identical configurations. Special attention was paid to the design of the openings. All the openings have a width equal to that of the box. The exit opening is located close to the heating plate, as shown in Fig. 2. The entrance opening, made in the partition, could be shifted vertically, in order to find its optimal location. In the glass box, by full closing of the partition, a "pocket" is formed in which the smoke could be accumulated in the visualization experiments. The smoke enters the box when a window in the partition is opened. The distance between the partition and the sidewall of the box is 50 mm, the height of the window is 50 mm, and the exit opening is also 50 mm wide.

3.2. Preliminary experiments

A number of preliminary experiments was performed in order to establish the heat-transfer coefficients for the walls and for the cover of the box.

The heat transfer coefficient of the walls was estimated in the following way: The pressed-wood cover

was removed. The box was covered on its top by a plate of insulating material, about three times thicker than the walls. Hot air was blown into the box by a fan for a relatively long period of time. The air blowing was stopped when the walls and the air inside the box reached a steady state. Then, cooling of the air inside the box took place through the walls only. The rate of heat lost was estimated from measurements of air temperature inside the box. The overall heat transfer coefficient was then obtained by using the mean air temperature in the box, the ambient air temperature, and the surface area of the walls.

The thermal resistance of the walls was then calculated from the overall heat transfer coefficient and the convection heat transfer coefficients inside and outside the box. The value of the convection heat transfer coefficient outside the box was obtained in our laboratory as 10–12 W/ m^2 °C. The value of the convection heat transfer coefficient inside the box was assumed in the range of 2–5 W/ m^2 °C. The heat transfer coefficient based on the thermal resistance of the wall and the convective resistance outside the box was obtained as 0.08 W/m^2 °C with an uncertainty of 15%. This value was used later in the numerical simulations. Evidently, the major thermal resistance pertains to the wall insulation.

The heat transfer coefficient for the cover plate was found in a similar way. The described above experiment was repeated, with the actual cover instead of the insulating material. Since the contribution of the walls had been established earlier, the heat transfer coefficient for the cover plate was found to be 5 W/m^2 °C, with an uncertainty of 20%. This value was used later in the numerical simulations.

3.3. Temperature measurements

Temperature measurements were conducted inside the cardboard box using the arrangement described above (Fig. 2). The measurements were continuously performed by the T-thermocouples using a data logger connected directly to a PC. The ambient air temperature was also continuously monitored, using a thermocouple identical to the thermocouples in the enclosure, and connected to the same PC. Since both the processes of heating and of ventilation were found to be slow, the time constant of thermocouples could not affect the results of the measurements significantly.

The readings of the thermocouples were verified exposing them simultaneously to the ambient air, while being connected to the data acquisitor. The time of exposure was 10–15 min. It was found that the maximum difference between the readings of any two thermocouples did not exceed 0.2°C.

Considering the system in question, one should bear in mind that there exists direct radiation heat transfer from the hot plate to the temperature-measurement devices. This well-known effect (see, for example, Eckert and Drake [11]) can cause a significant deviation of the thermocouple temperature from the temperature of the ambient air. In order to prevent the radiation error, we decided in the present investigation to suppress the radiation from the plate itself. A thin aluminum foil was glued to the plate carefully, in order to achieve maximum contact of the two surfaces. The outside surface of the foil is specular, and its emissivity, from the literature [11], is as low as 0.04.

The experiments inside the cardboard box were performed as follows:

The entrance and exit openings were closed tightly. The plate was heated by boiling water in the tank. Heat was transferred from the hot plate to the air inside the enclosure, and the latter was heated until a steady state was established. Then, the exit and entrance windows were opened simultaneously. Due to the ventilation, temperature fell down in the enclosure till a new steady state was achieved.

It took typically 1.5–2 h to achieve a steady state inside the closed box. In the open box, 1–1.5 h was needed to reach a steady state, varying with the entrance window position: 1 h for the bottom and mid-height openings; 1.5 h for the top opening. The thermocouples readings were taken every 15 min. The criterion used to infer a steady state was based on a 0.2°C variation during one hour in the reading of any thermocouple in the enclosure.

About 20 experiments were performed in the closed box at steady state. Several experiments were carried out for each position of the entrance window. The local excess temperatures, namely the temperatures above the ambient temperature, were recorded and displayed graphically. The temperature distribution was similar in all the cases.

A typical temperature distribution in a closed box at steady state is shown in Fig. 3(a). The excess temperature readings are displayed near each thermocouple. There are 16 points altogether in the core of the enclosure. This number is too few for constructing isotherms. However, by using Matlab 5.3 software, points of the same reading are connected by lines to show the trends of the temperature field.

Figs. 4(a), 5(a), 6(a) show the temperature distributions in the open box at steady state for the three positions of the entrance window. The measured excess temperature is displayed near each thermocouple. Again, points of the same reading are connected. The drawn lines show the trends of the temperature field.

3.4. Visualization

As mentioned above, visualization was performed in a transparent box of which dimensions were

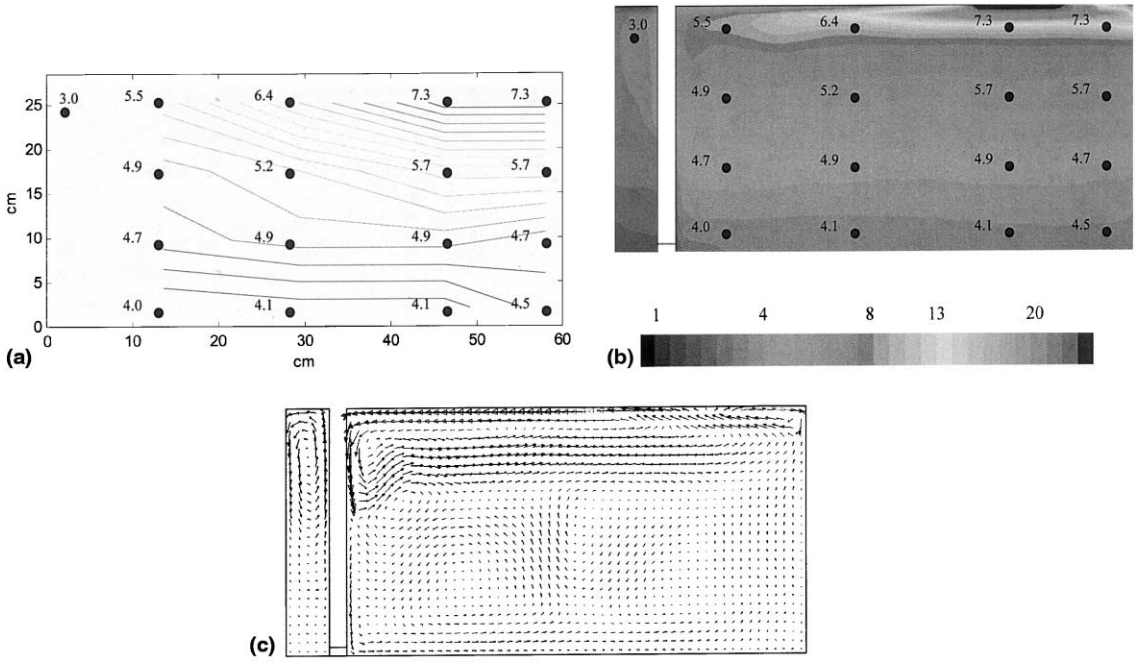

Fig. 3. Results for a steady state inside the closed box: (a) temperature measurements; (b) simulated temperature field at the vertical mid-plane; (c) simulated vector flow field at the vertical mid-plane.

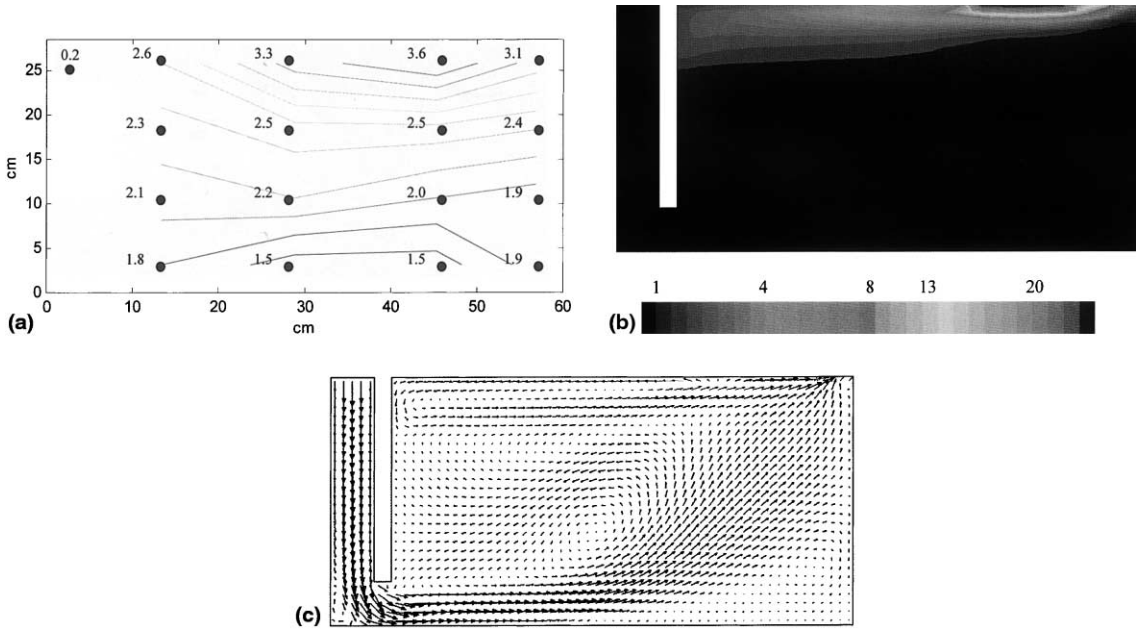

Fig. 4. Results for the ventilated steady state with the entrance opening at the bottom of the enclosure: (a) temperature measurements; (b) simulated temperature field at the vertical mid-plane; (c) simulated vector flow field at the vertical mid-plane.

identical to those of the cardboard box. The two objectives were: (1) to study the transient flow through the box at various positions of the entrance window, and (2) to study the transient process of gradual ventilation of the box at various positions of the entrance window.

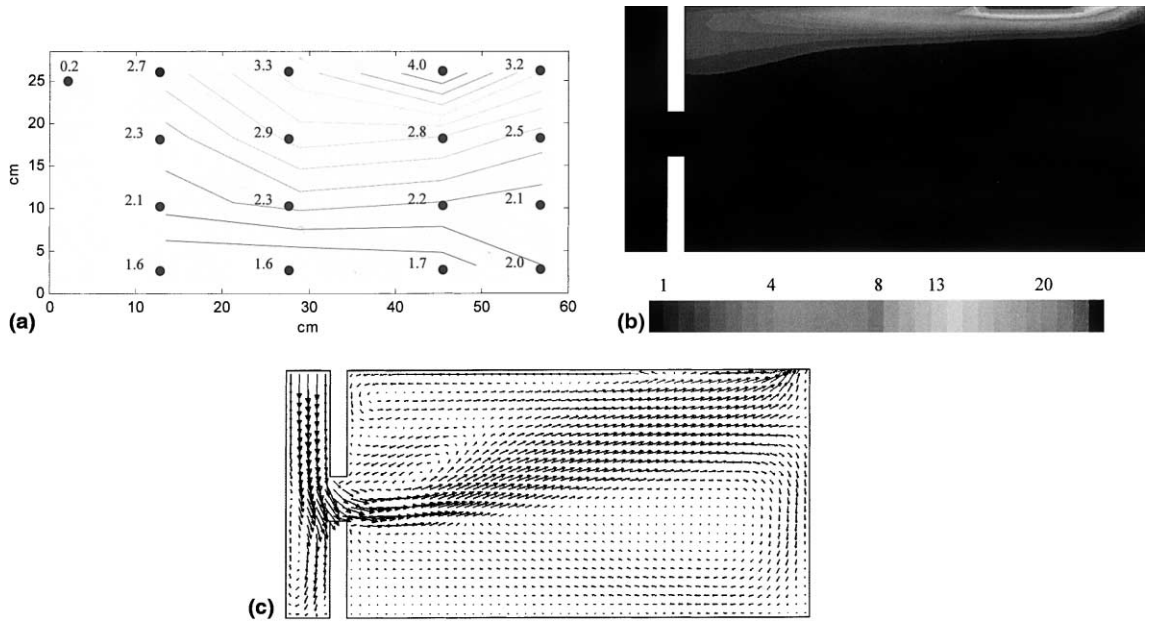

Fig. 5. Results for the ventilated steady state with the entrance opening at the half-height of the enclosure: (a) temperature measurements; (b) simulated temperature field at the vertical mid-plane; (c) simulated vector flow field at the vertical mid-plane.

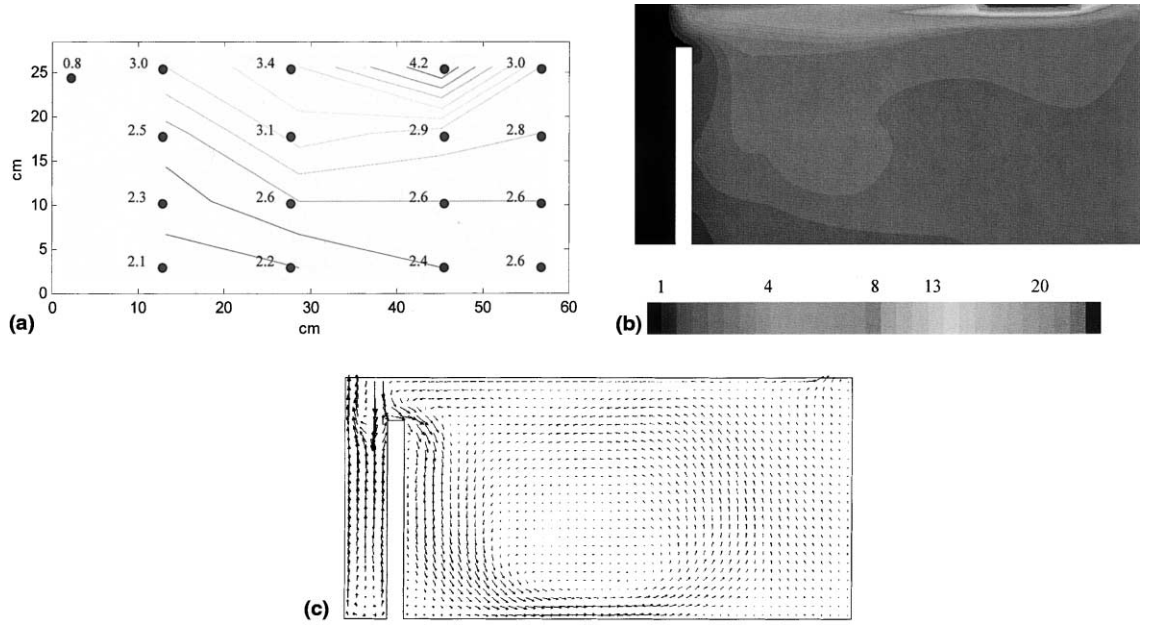

Fig. 6. Results for the ventilated steady state with the entrance opening at the top of the enclosure: (a) temperature measurements; (b) simulated temperature field at the vertical mid-plane; (c) simulated vector flow field at the vertical mid-plane.

Accordingly, two types of visualization experiments were performed:

1. Smoke flowing from the entrance to the exit through an initially clean, heated enclosure;
2. Clearing of the heated and initially filled with smoke enclosure.

Video recordings obtained during the experiments were carefully inspected in a playback mode, and

analyzed using a PC equipped with a frame-grabber and image processing software.

It is important to note that the glass walls have a thermal conductivity much larger than that of the walls of the insulated box. Thus, the thermal losses to the surroundings are much larger through the glass. For this reason, an uncovered hot plate was used in the visualization, where the additional heat input due to radiation compensated for the losses through the glass.

3.5. Flow of smoke through the box

A typical experiment with the smoke initially accumulated in the entrance pocket and then allowed to pass through the enclosure was performed as follows. The partition was closed fully, forming a pocket. Smoldering incense sticks were placed in the pocket. Then, the entrance and exit windows of the box were closed tightly. The smoke trapped behind the partition and the sidewall cooled down by transferring heat to the surroundings through the sidewall. In the meantime the enclosure was heated up to a steady state. Then, all the windows were opened simultaneously. The smoke flow into and through the box was observed and recorded by a video camera.

The results are shown in Fig. 7(a) for the entrance opening at the mid-height of the box. The frames were taken at 0, 2, 4, 6, 8, 10, 12, and 20 s after the opening of the system. The results, for the entrance opening at the bottom of the box, were reported in the previous investigation [8]. For the entrance at the top, the smoke mostly flew into the surroundings, and only a small amount of it entered the box.

3.5.1. Clearing the box

A typical experiment with the smoke initially accumulated in the whole box and then allowed to leave it through the windows was performed as follows: Smoldering incense sticks were placed in the box. Then, entrance and exit windows of the box were closed tightly. The enclosure was heated up to a steady state, while the produced smoke was accumulated inside it. Then, the exit and entrance windows were opened simultaneously. Inflow of fresh air into the box and outflow of smoke from it were observed and recorded by a video camera.

Gradual clearing of the glass box was reported in the previous investigation [8], for the entrance opening at the bottom of the box. The complete clearing of the box took 2.5, 3, and 3.5 min for the window at the bottom, mid-height, and top, respectively.

4. Numerical study

The numerical calculations were performed for (1) the steady state established when the entrance and exit windows are closed, (2) the ventilated steady state established when the entrance and exit windows are open, and (3) the transient process of ventilation which takes place between the states (1) and (2), by opening the windows.

The basic conservation equations were solved numerically, using the FLUENT 4.52 CFD software. The form of these equations is as follows [12]:

- continuity

$$\frac{\partial \rho}{\partial t} + \frac{\partial}{\partial x_{\mathrm{i}}}(\rho u_{\mathrm{i}}) = 0, \tag{1}$$

- momentum

$$\frac{\partial}{\partial t}(\rho u_i) + \frac{\partial}{\partial x_j}(\rho u_i u_j) = -\frac{\partial p}{\partial x_i} + \frac{\partial \tau_{ij}}{\partial x_j} + \rho g_i, \tag{2}$$

- energy

$$\frac{\partial}{\partial t}(\rho h) + \frac{\partial}{\partial x_i}(\rho u_i h) = \frac{\partial}{\partial x_i}\left(k\frac{\partial T}{\partial x_i}\right) + \frac{\partial p}{\partial t} + u_i\frac{\partial p}{\partial x_i} + \tau_{ij}\frac{\partial u_i}{\partial x_j}, \tag{3}$$

where ρ is the density, u_i is the velocity component in the i-direction, p is the static pressure, t is time, u_i is a Cartesian coordinate, τ_{ij} is the stress tensor, g_i is the gravitational acceleration the i-direction, h is the static enthalpy, k is the thermal conductivity, and T is the temperature. Since neither large viscous stresses nor compressibility effects were expected in the current problem, the viscous heating term $\tau_{ij}(\partial u_i/\partial x_j)$ was not activated [12].

Since the flow is buoyancy-driven, the momentum equation, Eq. (2), is redefined in FLUENT using the following relation for the vertical x_2-direction [12]:

$$p' = -\rho_0 g x_2 + p, \tag{4}$$

where ρ_0 is the reference density taken at 300 K and atmospheric pressure. The Boussinesq approximation was not used, and the density temperature relation was provided as an input.

The boundary conditions for the momentum equation are no-penetration, no-slip at all the boundaries. When an open state is considered, the pressure boundary condition $p' = 0$ is imposed at the openings.

The boundary conditions for the energy equation are based on the experimental parameters. The temperature of 100°C is imposed on the hot plate. For the other boundaries, FLUENT makes it possible to incorporate the heat transfer coefficients and the outside temperatures in the calculation of the inside temperature field. These coefficients were measured in the preliminary experiments.

When a state of an open enclosure is considered, the temperature of the surroundings is imposed at the

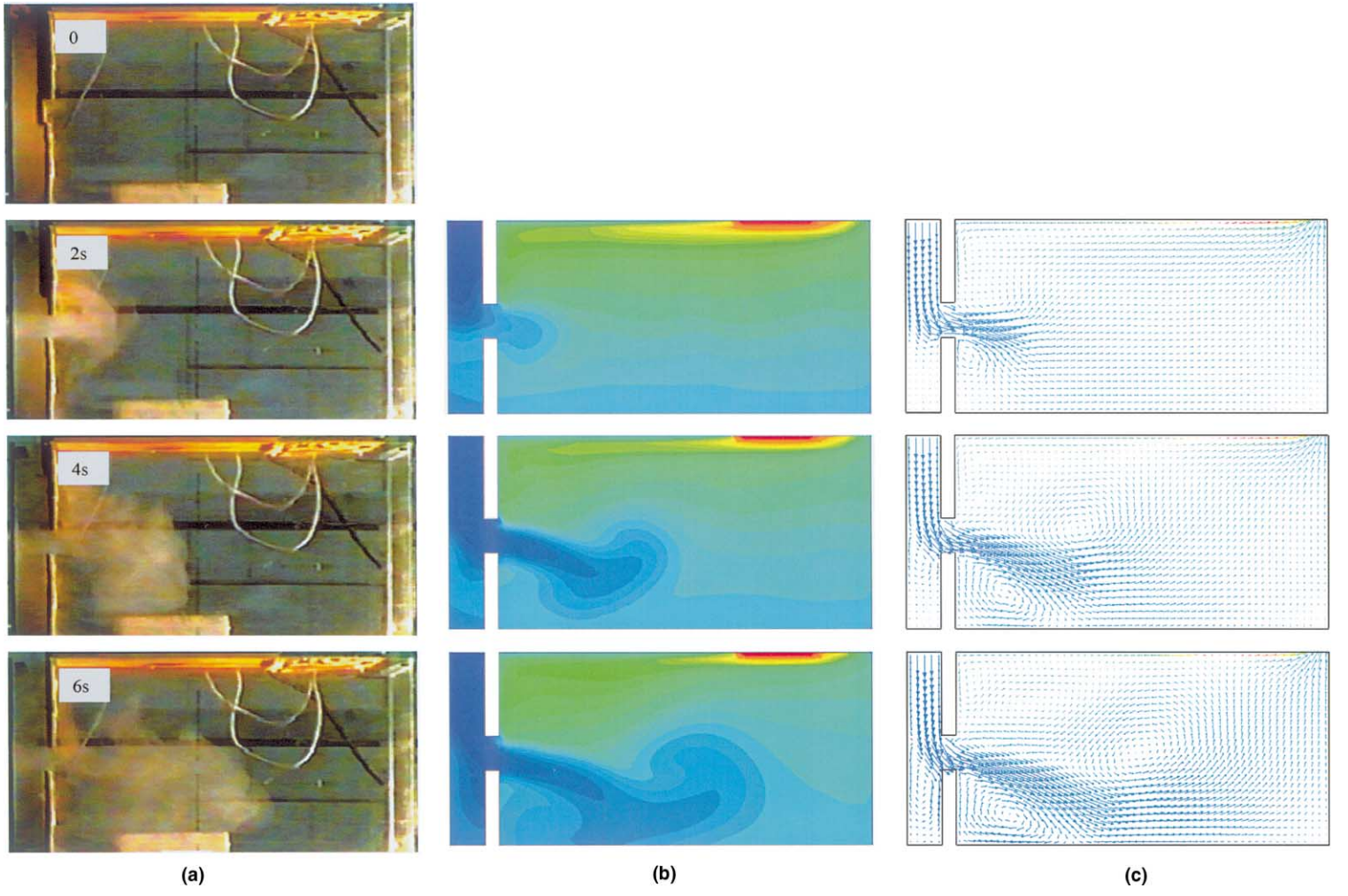

Fig. 7. Transient ventilation of the enclosure, for entrance window at the half-height of the box: (a) smoke visualization; (b) simulated temperature field at the vertical mid-plane; (c) simulated vector flow field at the vertical mid-plane.

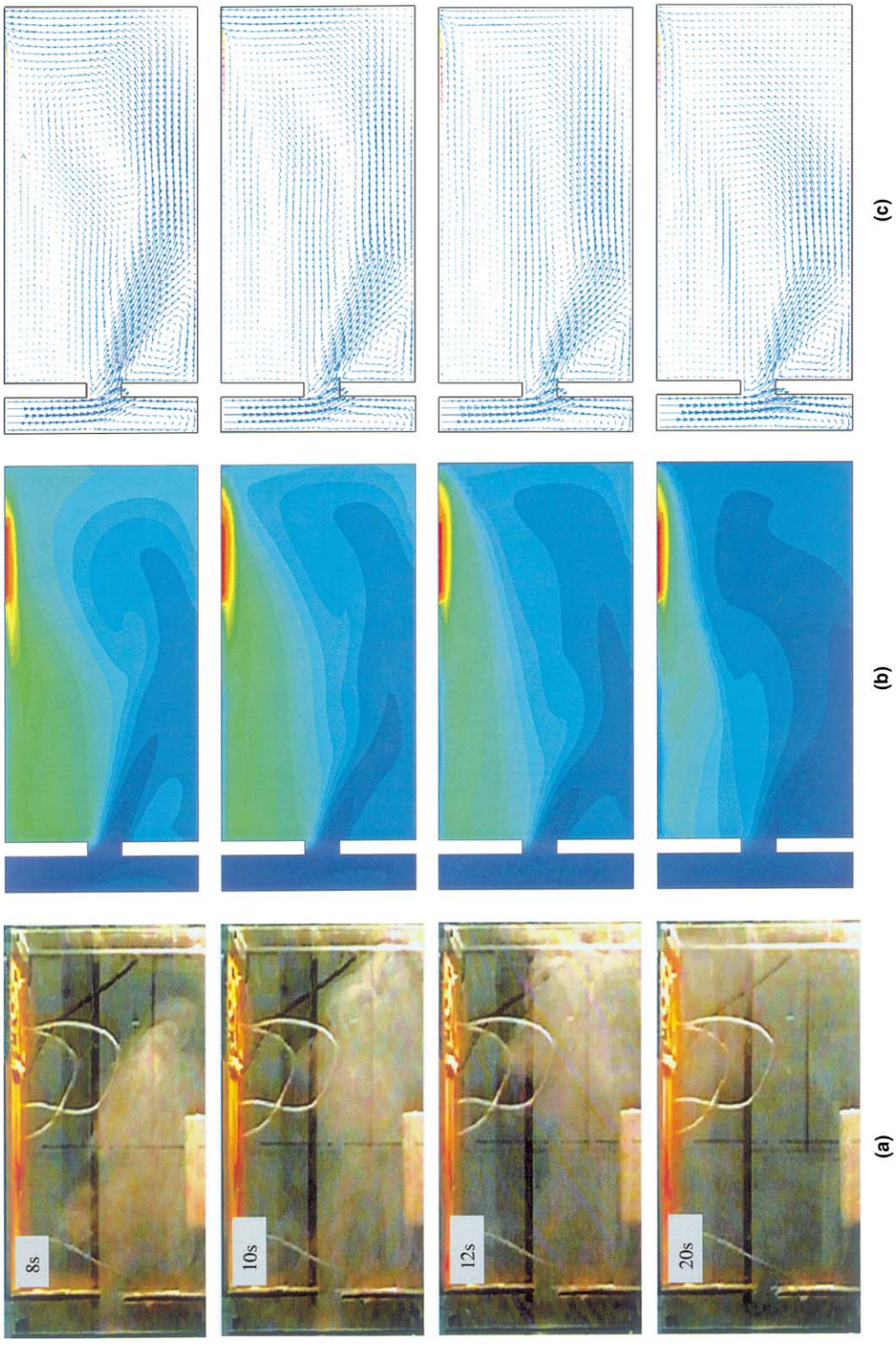

Fig. 7 (*continued*)

entrance opening. As for the exit opening, FLUENT adjusts the boundary condition there, extrapolating the temperature values from the interior grid cells adjacent to the exit.

Two-dimensional simulations were performed and reported in the previous investigation [8]. In the present study three-dimensional simulations are performed. The number of grids used was $60 \times 30 \times 8$ (length $\times$ height $\times$ width), where each cell was $1 \times 1 \times 3$ cm^3. The number of grids, both for the two-dimensional and three-dimensional simulations was chosen by its consequent refinement in the following way.

In the two-dimensional simulation we have defined an open box configuration and the position of the window at the bottom. The chosen cell was 1×1 cm^2, and the number of grids was 60×30. Then, the computation was repeated with a cell of 0.5×0.5 cm^2, and the number of grids was 120×60. The temperature distribution in both simulations was the same and unaffected by the cell size.

In the three-dimensional simulations we have again defined the same configuration of the box. We have chosen the cell size of $1 \times 1 \times 3$ cm^3, and the number of grids was $60 \times 30 \times 8$. Then, the computation was repeated with a cell of $1 \times 1 \times 1$ cm^3, and with the number of grids of $60 \times 30 \times 24$. The simulated temperatures were compared. The deviations obtained were within the range of 0.2°C, which is the uncertainty range of temperature measurements.

The heat transfer coefficients of the wall and cover, obtained with an uncertainty of 15 and 20%, respectively, as indicated earlier, affect the simulated temperatures in an open enclosure at steady state, up to 0.1°C. This value is again within the uncertainty range of measurements.

Fig. 3(b) shows the simulated temperature field, along with the measured temperatures, at steady state in the vertical mid-plane of the closed box. Fig. 3(c) shows the simulated vector flow field, at steady state, in the vertical mid-plane of the closed box.

The measured temperature distributions, the simulated temperature fields, and the flow fields are shown in Figs. 4–6 for the open box at steady state with the entrance window at the bottom, at the mid-height, and at the top of the box, respectively.

Fig. 7 represents the results of the three-dimensional simulations for transient processes, occurring when the initially closed box, operated at a steady state, is opened, using the mid-height window. Fig. 7(b) represents the temperature field, and Fig. 7(c) represents the vector flow field in the system, 2, 4, 6, 8, 10, 12, and 20 s after the windows have been opened. Fig. 8 represents a simulated initial stage of ventilation for the entrance window at the bottom of the box, at 1, 2, 4, 6, 8, 10, 12 and 20 s.

5. Results and discussion

5.1. Steady state – numerical results vs. measurements

Fig. 3(a) shows a typical temperature distribution for the steady state in the closed box. In all the experiments, the measured temperature inside the box, except for the region in the vicinity of the hot plate, was 4–7° above the ambient temperature. One can see that in the closed box, almost horizontal stratification exists. The only region where the distribution is different is, obviously, in the vicinity of the hot plate, because the latter is only a small part of the otherwise cold upper cover. We note that in the vicinity of the hot plate the temperature gradients are steep.

Fig. 3(b) shows the steady-state temperature field at the vertical mid-plane in the closed box, as found in the three-dimensional simulation. One can see that except for the vicinity of the upper cover, the temperature field is stratified, and distinct horizontal layers are displayed. This result is in agreement with the measurements and reflects the physical phenomena arising from heating by a downward-facing hot plate.

One can see from Fig. 3(b) that, except for the vicinity of the hot plate, the temperature inside is 4°C (light blue) to 7– 8°C (green) above the ambient temperature. Thus, there is a good agreement between the measured temperature distribution and the simulated temperature field. For convenience, the measured values are superposed on the simulated field. The difference between the average temperature calculated as the mean for 16 thermocouples, and the average temperature obtained from the numerical simulation for the same region, was as small as 0.1°C.

Fig. 3(c) shows the vector flow field at the vertical mid-plane for the closed box, as found in the three-dimensional simulation. From the simulated flow field one can see how the convective currents cause the temperature distribution. In particular, it is clear from Fig. 3(c) that the heated air moves from the hot plate mostly to the left, reflecting the asymmetry of the plate location.

Figs. 4(a), 5(a), 6(a) show the measured temperature distributions at steady states in an open box. The shape of the drawn isotherms reflects the differences caused by the changing location of the entrance window, which was at the bottom in Fig. 4(a), at the mid-height in Fig. 5(a), and at the top in Fig. 6(a). One can see that the temperature at any location inside the box is much lower in the open box than it is at the same location in the closed box. This means that the passive ventilation is quite effective. The mean temperature is slightly higher when the entrance window is at the upper part of the box.

Figs. 4(b), 5(b), 6(b) represent the steady-state temperature field at the vertical mid-plane in the open box

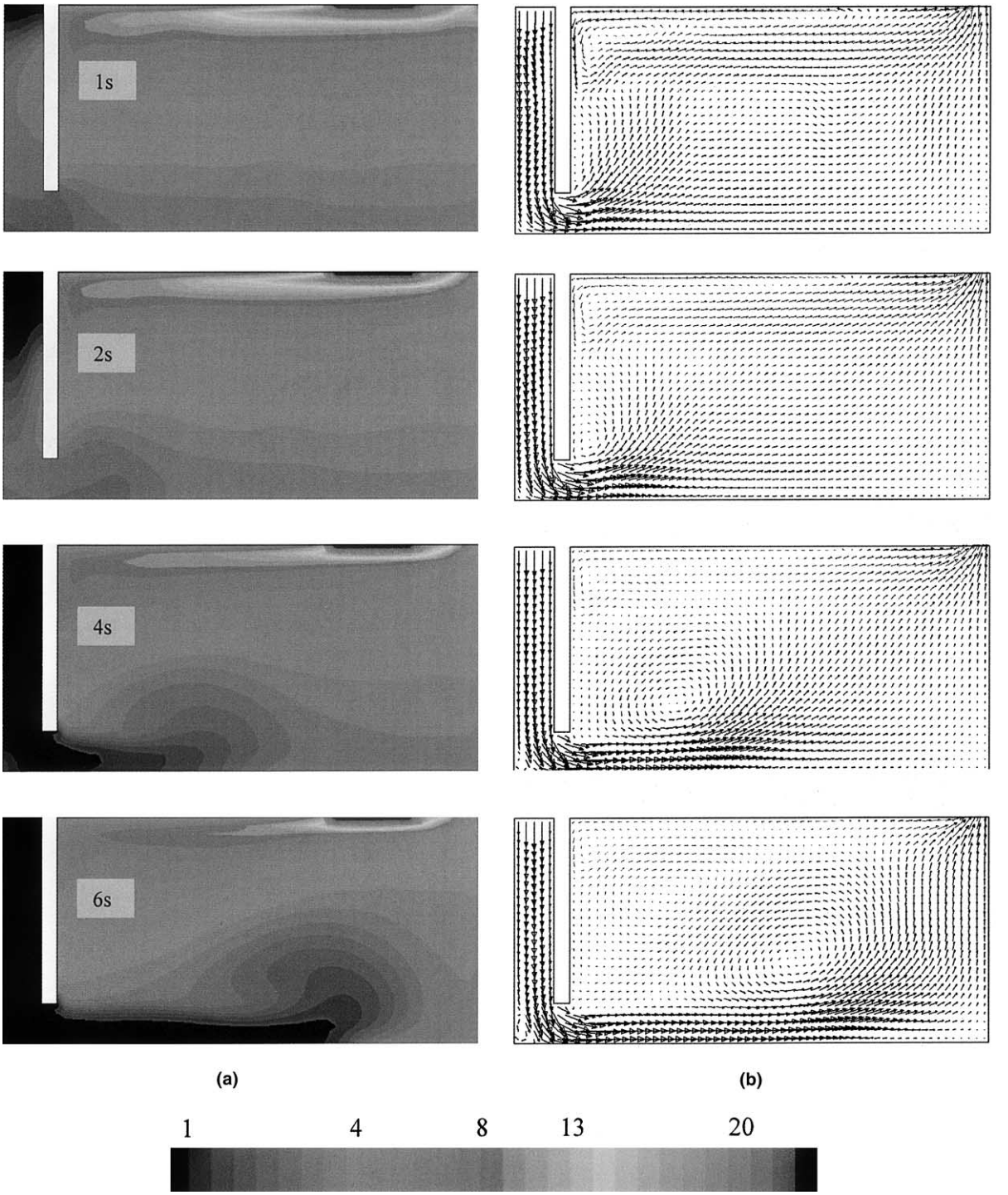

Fig. 8. Transient ventilation of the enclosure, for entrance window at the bottom of the box: (a) simulated temperature field at the vertical mid-plane; (b) simulated vector flow field at the vertical mid-plane.

with the entrance window positioned at the bottom, at the mid-height, and at the top of the box, respectively, as found in the three-dimensional simulation. The difference between the average temperature calculated as the mean for 16 thermocouples, and the average temperature obtained from the numerical simulation

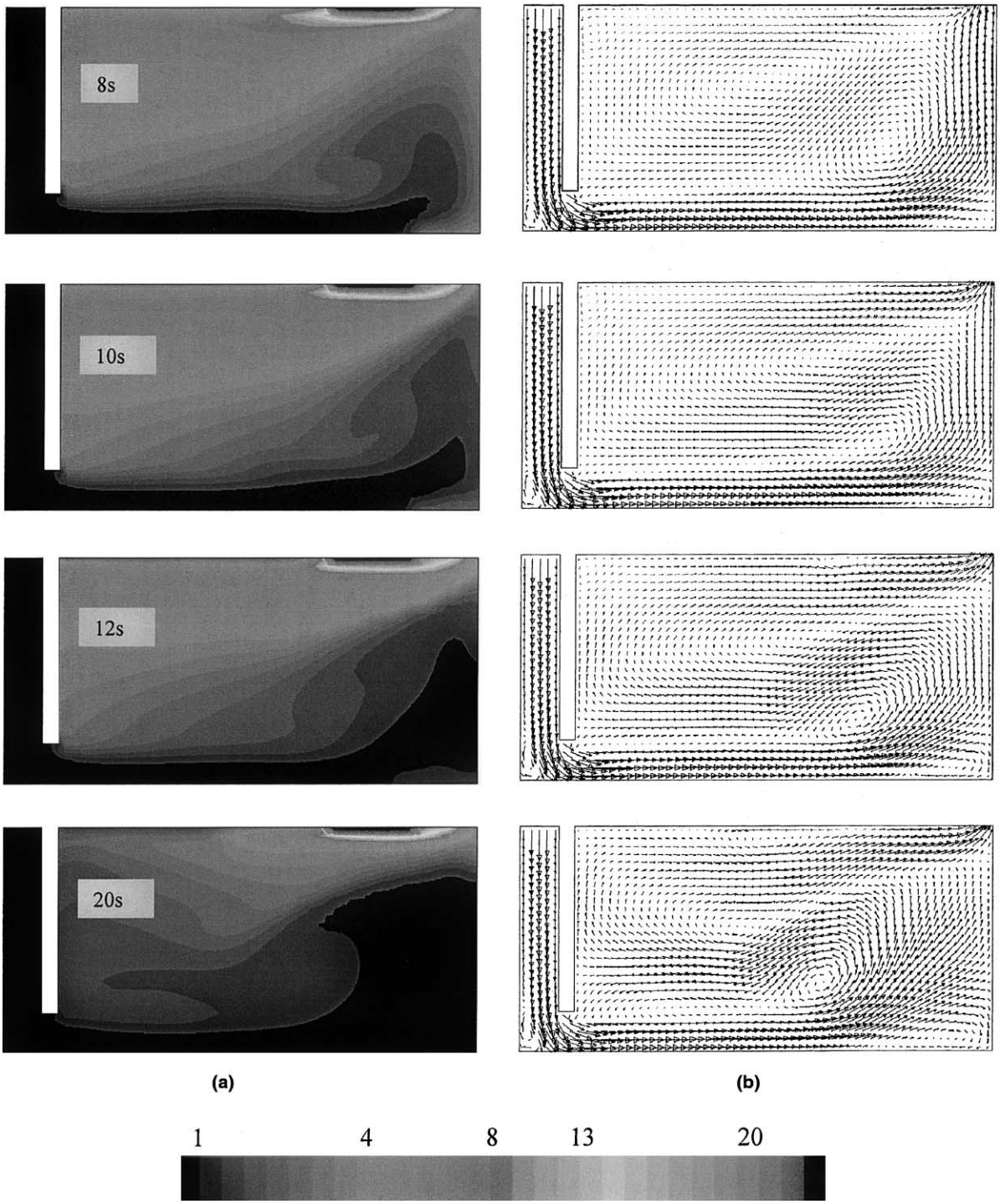

Fig. 8 (*continued*)

for the same region, was about 2°C for the entrance window at the bottom and at the mid-height of the box. In our opinion, this discrepancy is mostly due to the more intensive mixing of the warmer, upper vortex with the expanding air at its sharp-edged entrance.

A simulation for the entrance window positioned at the top of the box, shown in Fig. 6(b), indicates that in this case the temperature inside the box is higher. Here, the difference between the average temperature calculated as the mean for 16 thermocouples, and the average temperature obtained from the numerical simulation for the same region, was about 0.5°C. This discrepancy is smaller than in the bottom and mid-height configurations, because the numerical simulation "sees" the mixing of the warm vortex with the incoming stream of air, as shown in Fig. 6(c).

Figs. 4(c), 5(c), 6(c) show the vector flow fields at the vertical mid-plane for the open box, for various locations of the entrance window, as obtained in the three-dimensional simulation. Comparison of these with Figs. 4(b), 5(b), 6(b) shows how the flow through the enclosure alters the temperature distribution.

The uncertainty of the simulated temperatures due to the measured heat transfer coefficients is within the range of 0.2°C.

All the simulations were conducted in the laminar flow regime. The calculated Rayleigh number is $Ra = 12 \times 10^6$ for the natural convection from the hot plate at the conditions of the present investigation. This is within the laminar regime.

Analysis of the flow field shows that the induced flow velocities in the box are lower than 10 cm/s. Hence, the Reynolds number based on the length of the enclosure does not exceed the value of $Re_L = 4 \times 10^4$, and is below the respective critical value of 5×10^5 over a flat plate. However, the flow conditions inside a box are different from a flow over a flat plate, and turbulence may arise at expansions or contractions, as for example at the sharp-edged entrance window. Therefore, the Reynolds number along the "floor" not necessarily predicts a laminar regime.

5.2. Transient state – numerical results vs. visualization

Fig. 7(a) shows the results of the visualization for the entrance window at the mid-height of the box. The frames were taken at 0, 2, 4, 6, 8, 10, 12, and 20 s after the opening of the system. The results of visualization for the entrance window at the bottom were reported in the previous study [8].

Fig. 7 illustrates, in addition to the visualization, the three-dimensional simulation for the transient process occurring when the closed box, at steady state, is being opened using the mid-height window. Fig. 7(b) represents the temperature fields, and Fig. 7(c) shows the vector flow fields. The system is shown at 2, 4, 6, 8, 10, 12, and 20 s after opening the windows. Fig. 8 represents an example of the three-dimensional simulation of transient ventilation in a configuration with the entrance window at the bottom of the box, at 1, 2, 4, 6, 8, 10, 12, and 20 s.

Figs. 7 and 8, along with those presented in [8], show a remarkable agreement between the experimental and numerical results. For a window at the bottom, the visualization shows that the smoke flows mainly along the bottom of the box, while a part of it is dispersed by a secondary vortex, first at the lower part of the box, and later over the whole box. Then, the smoke is sucked from the box entirely. The same agreement exists also between the experimental and numerical results for the window at the mid-height of the box. In particular, there is a mushroom-like shape of the smoke cloud, while the smoke descends to the bottom of the box and is dispersed by vortices.

Fig. 7(b) shows a low-temperature region growing from the entrance window. This pattern corresponds to the inflow of fresh air from the surroundings, as seen in Figs. 7(a) and(c). A similar picture is observed when the window is at the bottom of the box. For the window at the top, however, the air flowed out both through the entrance and exit openings.

The two-dimensional simulations were reported in [8] for the transient ventilation with the entrance window at the bottom of the box. Since the stream function is defined for a two-dimensional geometry, we have obtained the simulated flow field in the form of streamlines. The agreement with the visualized images presented there was good. The three-dimensional simulations performed in the present work also agree very well with the visualized images.

5.3. Applicability to ventilation

The results obtained above allow us to reach two main goals. First, a comparison of the measurements and visualization with the computer simulations is important in order to assess the reliability of the numerical simulations for their present and further applications to other systems. Second, a comparison of the results achieved indicates the preferable configuration of the system.

It is expected that a turbulent flow regime would prevail in large real-size structures. However, the trends demonstrated in the laminar flow model would reappear in real-size models.

The flow rates of air through the enclosure (or room) are of major importance in design of ventilation systems. The calculated steady air throughputs were 5.9×10^{-4}, 6.3×10^{-4}, 4.6×10^{-4} kg/s for the entrance window at the bottom, at the mid-height, and the top, respectively. The simulated excess mean temperatures in the open enclosure at steady state were 0.7, 0.6 and 2.3°C for the entrance window at the bottom, at the mid-height, and at the top, respectively.

In the transient process of venting the enclosure, the bottom-window configuration was cleared at the fastest rate. The top-window configuration was cleared at the slowest rate.

The temperature measurements and the flow visualizations are agreeable with the numerical simulations. Therefore, the simulations can be performed for other parameters of the system, such as heat input, insulation, or geometry. For example, in our laboratory model, the top cover had a much lower thermal resistance than the other walls. In a real building, the roof may have a thermal resistance equal to that of the walls. Therefore, if we conduct the simulation for our open box at steady state, using a heat transfer coefficient of 0.08 W/ m^2 °C for all the walls, then the heat losses decrease and the air throughput is enhanced. We obtain in such case a throughput of 6.35×10^{-4}, 6.7×10^{-4}, and 4.9×10^{-4} kg/s for the entrance window at the bottom, at the mid-height, and the top, respectively. The throughput increase is 6–8% in comparison with the experimental rig. In the well-insulated box, the simulated respective excess mean temperatures were 0.9, 0.9 and 2.3°C, thus, up to 0.3°C higher in comparison with the simulated temperatures in the experimental box. Actually, only the upper layer of air, in the vicinity of the cover, was warmer and contributed to the mean temperature rise. The core of the enclosure was well ventilated and remained at the almost ambient temperature, like the one illustrated in Figs. 4(b), 5(b), 6(b).

We have also examined by simulation the effect of heat input into the enclosure by varying the hot plate temperature. The bottom-window configuration was used in the simulation of a box of which all walls were well insulated (a heat transfer coefficient of 0.08 W/m^2 °C was used). The following results were obtained: at the hot plate temperatures of 70, 100, 130, and 160°C the throughputs were 5.2×10^{-4}, 6.35×10^{-4}, 7.2×10^{-4}, and 7.8×10^{-4} kg/s, respectively. The respective excess mean temperatures of the enclosure were 0.6, 0.9, 1.2, and 1.5°C. As one can see, the throughput increases with heat input. The core of the enclosure remains well ventilated, however the stagnant upper layer of hot air, which is not replaced by the induced flow, becomes hotter at higher heat inputs from above.

Design of a similar ventilated system necessitates consideration of the induced flow field in the room, namely, the flow directions, velocities and the achievable throughput, the temperature distribution in the room, the mean temperature of the inhabited core of the room, and the thickness of the hot air layer at the ceiling. By analyzing Figs. 4(b), 5(b), 6(b), the top window configuration appears less suitable. Also its air throughput is lower, and the excess mean temperature is higher (1.6–1.7°C) than in the other configurations.

The configuration studied by us originated from our work on ventilation. However, the method and the results can be applied to other similar systems.

6. Closure

The results of the present study show that ventilation can be achieved inside an enclosure heated by a downward-facing hot plate. A great advantage of this system is that it spares the usually necessary mechanical work. Also, the heat needed for the ventilation may be achieved from the solar energy, which makes such a system attractive for remote and desert regions.

A comparison of the experimental results with the numerical simulations demonstrates that the latter can be used in the prediction of the flow field and temperature field inside the ventilated system, both for the steady state and for the transient processes, if the calculations are based on the actual heat-transfer parameters.

References

[1] K.T. Yang, Natural convection in enclosures, in: S. Kakac, R.K. Shah, W. Aung (Eds.), Handbook of Single-Phase Convective Heat Transfer, Wiley, New York, 1987.
[2] S. Ostrach, Natural convection in enclosures, ASME J. Heat Transfer 110 (1988) 1175–1190.
[3] R.A.W.M. Henkes, C.J. Hoogendoorn (Eds.), Turbulent Natural Convection in Enclosures – A Computational and Experimental Benchmark Study, Editions Europeennes Thermique et Industrie, 1993.
[4] G.P. Mercier, Y. Jaluria, Fire-induced flow of smoke and hot gases in open vertical enclosures, Exp. Thermal Fluid Sci. 19 (1999) 77–84.
[5] T.S. Fisher, K.E. Torrance, Experiments on chimney-enhanced free convection, ASME J. Heat Transfer 121 (1999) 603–609.
[6] E. Yu, Y. Joshi, A numerical study of three-dimensional laminar natural convection in a vented enclosure, Int. J. Heat Fluid Flow 18 (1997) 600–612.
[7] I. Sezai, A.A. Mohamad, Natural convection from a discrete heat source on the bottom of a horizontal enclosure, Int. J. Heat Mass Transfer 43 (2000) 2257–2266.
[8] S. Druckman, E. Moshka, V. Dubovsky, R. Letan, Y. Weiss, G. Ziskind, Visualization of natural convection inside a ventilated enclosure, in: Proceedings of the Ninth International Symposium on Flow Visualization, Edinburgh, 2000 (paper No. 83).
[9] C.E. Kwak, T.H. Song, Natural convection around horizontal downward-facing plate with rectangular grooves: experiments and numerical simulations, Int. J. Heat Mass Transfer 43 (2000) 825–838.
[10] R.J. Goldstein, K.S. Lau, Laminar convection from a horizontal plate and the influence of plate-edge extensions, J. Fluid Mech. 129 (1983) 55–75.
[11] E.R.G. Eckert, R.M. Drake, Analysis of Heat and Mass Transfer, McGraw-Hill, New York, 1972.
[12] FLUENT User's Guide, Version 4.52, Fluent Incorporated.